

Quantum Critical Point at Finite Doping in the 2D Hubbard Model: A Dynamical Cluster Quantum Monte Carlo Study

N. S. Vidhyadhiraja*

Theoretical Sciences Unit,

*Jawaharlal Nehru Centre for Advanced Scientific Research,
Jakkur, Bangalore 560064, India.*

A. Macridin, C. Sen, M. Jarrell,[†] and Michael Ma
University of Cincinnati, Cincinnati, Ohio, 45221, USA

(Dated: November 2, 2018)

We explore the Matsubara quasiparticle fraction and the pseudogap of the two-dimensional Hubbard model with the dynamical cluster quantum Monte Carlo method. The character of the quasiparticle fraction changes from non-Fermi liquid, to marginal Fermi liquid to Fermi liquid as a function of doping, indicating the presence of a quantum critical point separating non-Fermi liquid from Fermi liquid character. Marginal Fermi liquid character is found at low temperatures at a very narrow range of doping where the single-particle density of states is also symmetric. At higher doping the character of the quasiparticle fraction is seen to cross over from Fermi Liquid to Marginal Fermi liquid as the temperature increases.

Introduction- The unusual properties of the hole doped cuprate phase diagram, including a pseudogap (PG) at low doping, and unusual metallic behavior at higher doping have lead many investigators to propose that there is a quantum critical point in the cuprate phase diagram at optimal doping. Different investigators argue that the PG is related with the establishment of order [1, 2, 3, 4, 5], where the optimal doping is in the proximity of the quantum critical point (QCP) associated with this order [4]. Other investigators argue that the QCP is located at the transition from a non-Fermi liquid (NFL) to Fermi liquid (FL) ground state without the establishment of order in PG region[6].

In previous work employing cluster extensions of the Dynamical Mean Field, a PG region was found at low doping in the two-dimensional Hubbard model. It is characterized by a narrow gap-like feature in the single-particle density of states, a suppression of the spin susceptibility, and a self energy of NFL character[8, 9, 10, 11, 12, 13].

In this paper, we employ significantly larger clusters than most previous studies, which affords us greater momentum resolution. We investigate the single particle properties of the two-dimensional Hubbard model with the dynamical cluster approximation (DCA) [14, 15]. We find further evidence for a QCP and are able to determine its character as the terminus of a Marginal Fermi Liquid (MFL) region, which separates a NFL PG region at low doping from a FL region at high doping. We present a comparative discussion of a few existing scenarios for quantum criticality in the context of our results.

Formalism- We consider a 2D Hubbard Hamiltonian

$$H = - \sum_{\langle ij \rangle \sigma} t(c_{i\sigma}^\dagger c_{j\sigma} + h.c.) + \epsilon \sum_{i\sigma} n_{i\sigma} + U \sum_i n_{i\uparrow} n_{i\downarrow} \quad (1)$$

where t is the hopping matrix, $c_{i\sigma}^\dagger (c_{i\sigma})$ is the creation (annihilation) operator for electrons on site i with spin σ , and U is the on-site Coulomb repulsion which is taken to be three quarters of the bandwidth $W (= 8t)$. The hopping t is restricted to nearest neighbors $\langle ij \rangle$.

We employ the DCA with a quantum Monte Carlo algorithm as the cluster solver. The DCA is a cluster mean-field theory which maps the original lattice model onto a periodic cluster of size $N_c = L_c^2$ embedded in a self-consistent host. Spatial correlations up to a range L_c are treated explicitly, while those at longer length scales are described at the mean-field level. However the correlations in time, essential for quantum criticality, are treated explicitly for all cluster sizes. To solve the cluster problem we use the Hirsch-Fye quantum Monte Carlo method[9, 16] and employ the maximum entropy method[17] to calculate the real frequency spectra.

A number of the normal state anomalies in the cuprates are describable by a MFL in proximity to a quantum critical point at finite doping[2]. The imaginary part of the MFL self energy has the form

$$\Sigma''_{MFL}(\omega) = -\alpha \max(|\omega|, T) . \quad (2)$$

In contrast the imaginary part of the FL self energy has the form

$$\Sigma''_{FL}(\omega) = -\alpha \max(\omega^2, T^2) \quad (3)$$

which would be expected to be valid at large doping and low temperatures. In the doping region beyond but near the QCP, the single particle properties of the model are observed to cross over from FL to MFL as the temperature crosses T_X and the frequency ω_x , we find that this may be fit with the form

$$\Sigma''_X(\omega) = \begin{cases} -\alpha \omega_x \max(|\omega|, T) & \text{for } |\omega| > \omega_x \text{ or } T > T_X \\ -\alpha \max(\omega^2, T^2) & \text{for } |\omega| < \omega_x \text{ and } T < T_X \end{cases} \quad (4)$$

Causality requires that $\alpha > 0$, and the integrals over these forms for the self energy are cutoff at ω_c which is of the order of the bandwidth $W(= 8t)$.

To compare our Matsubara frequency results to these forms of the real-frequency self energy[18], we transform each of these forms to Matsubara frequency using the transform of the non-Hartree part of the self energy

$$\Sigma(i\omega_n) = - \int \frac{d\omega}{\pi} \frac{\Sigma''(\omega)}{i\omega_n - \omega} \quad (5)$$

and then evaluate

$$Z_0(\mathbf{k}) = (1 - \text{Im}\Sigma(\mathbf{k}, i\omega_0)/\omega_0)^{-1} \quad (6)$$

where $\omega_0 = \pi T$ is the lowest Fermion Matsubara frequency. For a well behaved self energy, $\lim_{T \rightarrow 0} Z_0(\mathbf{k}) = Z(\mathbf{k})$ is the quasiparticle renormalization factor. For example, for the MFL, we find[18]

$$\frac{\Sigma_{MFL}(\mathbf{k}, i\omega_0)}{\omega_0} = \frac{\alpha}{\pi} \left[\ln \left(\frac{(\pi^2 + 1)T^2}{\pi^2 T^2 + \omega_c^2} \right) - \frac{2}{\pi} \tan^{-1} \frac{1}{\pi} \right]. \quad (7)$$

While for the FL, we find

$$\frac{\Sigma_{FL}(\mathbf{k}, i\omega_0)}{\omega_0} = \frac{-2\alpha T}{\pi} \left(\frac{\omega_c}{T} + 0.066235 - \pi \tan^{-1} \frac{\omega_c}{\pi T} \right) \quad (8)$$

when $T < \omega_c$. The crossover form is more complicated, but can be constructed from the same integrals used to derive Eqs. 7 and 8

$$\begin{aligned} \left(-\frac{\pi}{2\alpha} \right) \frac{\text{Im}\Sigma(i\omega_0)}{\omega_0} &= T\Theta(T_X - T) \left[\frac{\omega_x}{T} + 0.06623 \right. \\ &- \left(0.308 \frac{\omega_x}{\pi T} + \pi \tan^{-1} \frac{\omega_x}{\pi T} \right) - \frac{\omega_x}{2T} \ln \left(\frac{\omega_x^2 + \pi^2 T^2}{(1 + \pi^2)T^2} \right) \Big] \\ &+ \omega_x \left[0.0981 + \frac{1}{2} \ln \left(\frac{\omega_c^2 + \pi^2 T^2}{(1 + \pi^2)T^2} \right) \right]. \end{aligned} \quad (9)$$

The parameters, α , ω_c , T_X , and ω_x are determined from a fit to the quantum Monte Carlo data.

Results- We will present results for the model with $U = 1.5$ with bare bandwidth $W = 2$ setting the energy unit, and a 4×4 cluster. With this choice of U/t and cluster we are able to access low temperatures $T \gtrsim 0.01$ before the average sign of the sampling weight falls below 0.05. The low energy scales in the problem are the antiferromagnetic exchange energy J near half filling, the PG temperature T^* in the PG region, and the effective Fermi energy T_X at higher doping. As described previously[19], we can extract the effective near neighbor spin exchange energy J_{eff} from the spin excitation spectrum at $\mathbf{K} = (0, \pi)$. At this wavevector the magnon peak is expected at frequency $\omega \approx 2J_{eff}$. From this analysis, we find that $J_{eff} \approx 0.11$ for $N = 0.95$ and $N = 1$. The energy scales T^* and T_X are extracted from fits to the data presented below. It is important to note that in each of these fits, we include data for $T \ll J_{eff}$.

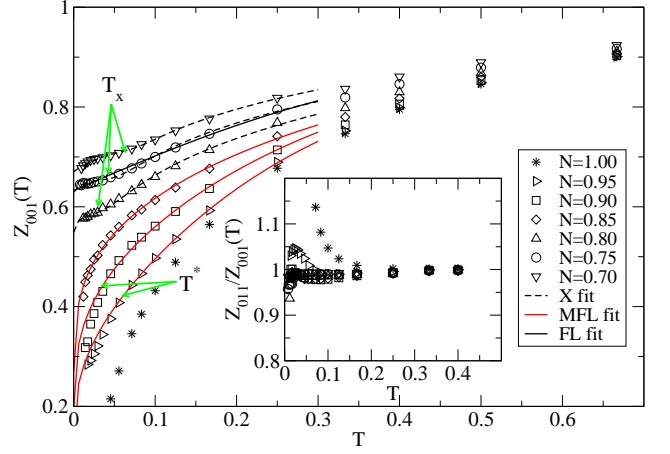


FIG. 1: Matsubara quasiparticle fraction $Z_0(\mathbf{k})$ versus temperature T evaluated with \mathbf{k} on the Fermi surface along the $(0, 1)$ direction for different fillings N when $U = 1.5$ and the bandwidth $W = 2$. The lines represent fits in the region $T < 0.3$ to either the MFL form, Eq. 7, for $N \geq 0.85$ or the crossover form (X), Eq. 9, for $N < 0.85$. The arrows indicate the values T_X extracted from the crossover fits or T^* (c.f. Figs. 3 and 4). Note that the data for $N = 0.85$ fits the MFL nearly perfectly, while the data for $N > 0.85$ is poorly fit by the MFL for $T < T^*$ which is too slow in temperature to provide a good fit due to the formation of the pseudogap. The data for $N = 0.75$ was also fit by the FL form, Eq. 8; however, the fit is clearly worse than that obtained by the crossover form. Inset: The ratio, Z_{011}/Z_{001} , is plotted as a function of temperature for different fillings. The ratio is essentially the same for all fillings at the QCP, indicating that Z is essentially isotropic, and becomes progressively more anisotropic as we dope into the PG region.

The Matsubara quasiparticle fraction is calculated with \mathbf{k} on the Fermi surface defined by the maximum $|\nabla n(\mathbf{k})|$ along the $(1, 1)$ and $(0, 1)$ directions. We will present detailed results and analysis for the latter only as we are interested in the crossover from PG to FL behavior, and the PG is stronger along the $(0, 1)$ direction. Z_{001} is shown in the main panel in Fig. 1 for $U = 1.5$ in units where $W = 2$ for different fillings.

The low temperature Matsubara quasiparticle data changes character as the filling N increases through $N = 0.85$. The data for $N > 0.85$ has negative curvature at all T . Whereas the data for $N < 0.85$ has negative curvature at high T , a region of weak positive curvature is found at lower T . The change in curvature of the low temperature data for $N < 0.85$ is easily understood as a crossover to a FL region. In a FL at zero temperature $Z_{0FL}(0) = 1/(1 + 2\alpha\omega_c/\pi)$ while for low T , $Z_{0FL}(T) \approx Z_{0FL}(0)(1 + 3.099\alpha Z_{0FL}(0)T)$. Since $\alpha Z_{0FL}(0) > 0$, $Z_{0FL}(T)$ at low T has a finite intercept and a linear region with positive initial slope indicative of FL formation. The next correction, of order T^2 , is small for $Z_{0FL}(0) \approx 0.6$ so that $Z_{0FL}(T)$ is a nearly lin-

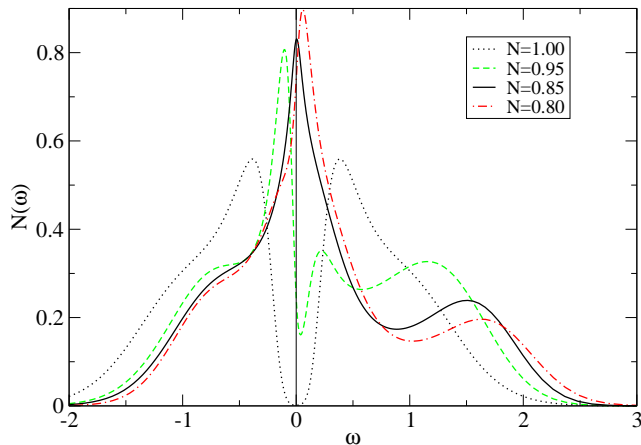


FIG. 2: The single-particle density of states (DOS) when $U = 1.5$, $W = 2$, and $T = 0.01429$. Note that the low-energy DOS is roughly symmetric around $\omega = 0$ for the critical filling $N = 0.85$ where $Z_0(\mathbf{k})$ fits a MFL form. This is consistent with the observation of rough particle-hole symmetry in the cuprates in the proximity of optimal doping[6].

ear function when fit to the low T data. On the other hand, the MFL always has negative curvature, as can be seen from an expansion of Eqs. 7 and 6 to second order in T . So at the transition between FL and MFL, a region of positive curvature is found at $T \approx T_X$. The data for $N < 0.85$ is well fit by the crossover form posed above, but is poorly fit by a FL form over the fitting region (see e.g., the solid line fit to the $N = 0.75$ data). When the data at $N = 0.85$ is fit with the crossover form for the $Z_{0X}(T)$, the fitting routine returns $\omega_x = T_X = 0$ (within the precision of the fit and data), consistent with the formation of a MFL. So the solid line shown in the plot is a MFL fit. The MFL fit to the $N = 0.85$ data is very good. In fact the quality of this fit was better than that obtained for any of the fitting forms to any of the other data sets, despite the fact that the MFL form only has two adjustable parameters. In order to show that the conclusions from the above analysis are not specific to the direction $(0, 1)$, we plot the ratio, Z_{011}/Z_{001} , in the inset of Fig. 1 as a function of temperature for different fillings. The ratio is seen to be essentially the same for all fillings at the QCP, indicating that Z is essentially isotropic at the QCP, and becomes progressively more anisotropic as we dope into the PG region.

The data with $N = 0.85$ in some other ways is special. For example, at this filling the low temperature single-particle density of states (DOS), which is plotted in Fig. 2 for several fillings, is peaked at zero frequency. At low energies $|\omega| \lesssim J_{eff}$ the $N = 0.85$ DOS is nearly symmetric around this point. This is consistent with the observation of particle-hole (p-h) symmetry in the transport of the cuprates at optimal doping[6].

In order to characterize the region $N > 0.85$, the PG

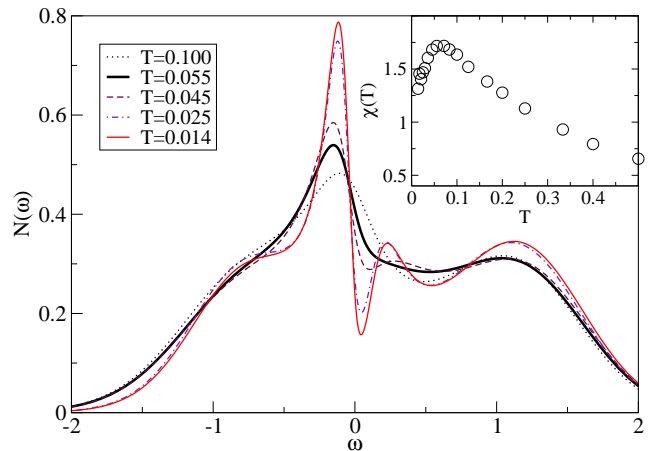


FIG. 3: The single-particle density of states in the pseudogap region for various temperatures with $N = 0.95$, $U = 1.5$, $W = 2$. Inset: The bulk, $\mathbf{Q} = 0$, cluster susceptibility for the same parameters. The PG in the DOS begins to develop at roughly the same temperature T^* which identifies the peak susceptibility.

region, we also explored the temperature dependence of the DOS and the bulk ($\mathbf{Q} = 0$) spin susceptibility of the cluster, as shown in Fig. 3 and its inset, respectively. We find a concomitant depression of the low energy DOS at temperatures below the peak in the susceptibility. The suppression of the susceptibility indicates the suppression of low energy spin excitations. $Z_{001}(T)$ in this region is well fit for $T > T^*$ (see Fig. 4) by the MFL form, but is poorly fit by the MFL form for $T < T^*$, as shown in Fig. 1. The MFL form changes too slowly with decreasing T , due to the formation of the PG for $T < T^*$.

The relevant temperatures near the QCP, T_X and T^* , are shown in Fig. 4. The PG temperature was determined from the peak in the susceptibility and the initial appearance of the PG in the DOS as shown in Fig. 3, and T_X from the fit to Eq. 9.

We also explored the effect of larger clusters and U/t ; however, these results are restricted by computational limitations including, especially, the minus sign problem. Despite this, some calculations were possible for $N_c = 24$ site clusters. For the same parameters used above, we find that the PG temperature T^* increases slightly near half filling. The critical filling where the $Z_{001}(T)$ is best fit by a MFL, the DOS is p-h symmetric at low frequencies remains between $N \approx 0.85$ to $N \approx 0.86$. Due to the minus sign problem, we did not have enough low temperature data to determine the crossover temperature precisely for clusters with $N_c = 24$. We also explored larger values of $U = W = 2$ for the $N_c = 16$ cluster (this data was produced in an earlier study). Again conclusions are limited by the minus sign problem; however, we find that the PG vanishes at roughly $N = 0.78$, consistent with optimal doping in the cuprates[6], and at this filling

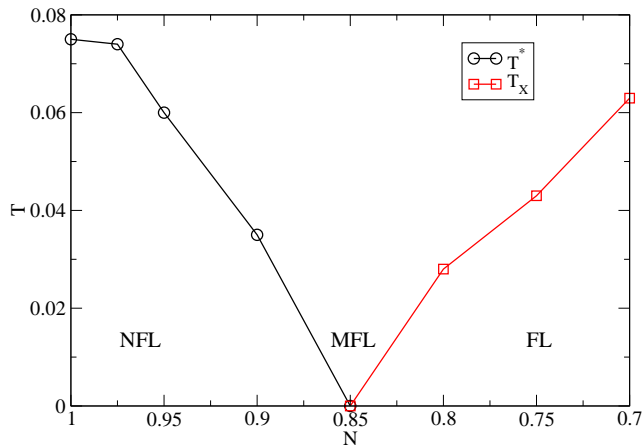


FIG. 4: The pseudogap temperature T^* , identified from the peak in the susceptibility and the emergence of the PG in the DOS shown in Fig. 3 and the FL to MFL crossover temperature identified by fitting Eq. 9 to the Matsubara quasiparticle data shown in Fig. 1.

the DOS is again p-h symmetric at low energies.

Discussion- Several different scenarios have been proposed to explain the transition from PG to FL behavior and the strange behavior seen near optimal doping in the cuprates such as the MFL phenomena.

An extension of the bond-solid scenario [4, 5, 20] is consistent with our results. Here, a bond-solid is conjectured to coexist with the pseudogap in the underdoped region, and the QCP marks the doping where the transition temperature to bond order vanishes. We suggest that the NFL behavior could be due to the scattering of quasiparticles from bond excitations. For dopings greater than, but near, the PG region, there would be remnant bond excitations. The low energy scale of these excitations will be cut off by the finite correlation length of the bond order, yielding a gap to bond excitations. So low energy quasiparticles may form a FL, while higher energy ones do not due to scattering from these bond excitations. In this scenario, the gap to bond excitations is proportional to T_X , which presumably will grow as the bond correlation length falls as the system is doped away from the QCP. One problem with this scenario is that it requires gapless bond excitations in the PG region, but due to the finite size of the cluster there should be a gap which scales with the cluster size. However, this gap may be small so its effects might not be seen at the temperatures we can access.

The spectral-weight transfer scenario[6, 21] also provides a consistent interpretation. In a hole-doped Mott insulator, with doping $x = 1 - N$ and large U/t , each doped hole yields two states immediately above the chemical potential. One comes from the lower and the other from the upper Hubbard band. When the system is doped so that the number of low-energy states (i.e., not

including those in the upper band) above and below the chemical potential are equal, so that $2x = 1 - x$ or $x = 1/3$, then p-h symmetry is obtained. For finite U/t , the critical doping for p-h symmetry is smaller[6]. This scenario also provides a general mechanism for the breakdown of the FL in the PG region[22]. In a FL there is a one-to-one correspondence between the particles and quasiparticles which means that the number of ways of adding a particle at low energies equals the number of ways that one can add an electron to the unoccupied states. This correspondence breaks down in the PG region since the number of ways to add an electron is $2x$, while the number of ways one can add a particle is larger[6]. Since such an argument relies on the asymmetry of adding a hole or an electron, it is clearly invalid when p-h symmetry is achieved for the low energy states. Thus this scenario explains the p-h symmetry of the DOS at the QCP, as found in Fig. 2.

Our results differ from previous extended DCA results for the t-J model on a $N_c = 4$ cluster where a FL-FL crossover, with maximum scattering is found at a critical point not associated with MFL behavior[7]. It is not clear whether the model or the method is responsible for these differences, although note that the spectral-weight transfer arguments discussed above suggest FL physics for the t-J model even at small doping[22].

Conclusion- We investigate the Matsubara quasiparticle fraction on the Fermi surface and the PG of the two-dimensional Hubbard model. As a function of doping, $Z_{001}(T)$ changes character. For doping beyond the critical point, as the temperature is lowered the curvature of $Z_{001}(T)$ changes from negative to positive. This can be understood as a change from a MFL to a FL as T falls. At lower doping, the curvature is negative for all T , including $T \ll J_{eff}$, consistent with a NFL state. A PG is also found in the DOS and the bulk spin susceptibility at lower doping. At the QCP which separates these two regions, we find a MFL which is also found for $T > T^*$ and $T > T_X$.

This research was supported by NSF DMR-0312680, DMR-0706379 (MJ and NSV), IUSSTF (NSV), DOE CMSN DE-FG02-04ER46129 (AM), and by the DOE SciDAC grant DE-FC02-06ER25792 (CS and MJ). Supercomputer support was provided by the Ohio Supercomputer Center. We would like to thank R. Gass, P. Phillips and M. Vojta for useful conversations.

* Electronic address: raja@jncasr.ac.in

† Electronic address: jarrell@physics.uc.edu

- [1] S. Chakravarty, R. B. Laughlin, D. K. Morr, and C. Nayak, Phys. Rev. B **63**, 094503 (2001).
- [2] C. M. Varma, Phys. Rev. Lett. **83**, 3538 (1999).
- [3] S. Kivelson, E. Fradkin, and V. Emery, Nature (London) **393**, 550 (1998).

- [4] M. Vojta, Y. Zhang, and S. Sachdev, Phys. Rev. B **62**, 6721 (2000).
- [5] S. Sachdev, Rev. Mod. Phys. **75**, 913, (2003); S. Sachdev, Nature Physics, **4**, 173 (2008).
- [6] S. Chakraborty, D. Galanakis, P. Phillips, preprint, arXiv:0807.2854.
- [7] K. Haule and G. Kotliar, Phys. Rev. B **76**, 092503 (2007).
- [8] M. Jarrell, Th. Maier, M. H. Hettler, and A. N. Tahvildarzadeh, EuroPhysics Letters, **56** pp563-569 (2001).
- [9] M. Jarrell, Th. Maier, C. Huscroft, and S. Moukouri, Phys. Rev. B **64**, 195130 (2001).
- [10] A. Macridin, M. Jarrell, Thomas Maier, P. R. C. Kent, and Eduardo D'Azevedo, Phys. Rev. Lett. **97** 036401 (2006).
- [11] D. Sénéchal and A. -M. S. Tremblay, Phys. Rev. Lett. **92**, 126401 (2004).
- [12] T. -P. Choy and P. Phillips, Phys. Rev. Lett. **95**, 196405 (2005).
- [13] A. -M. S. Tremblay, B. Kyung and D. Sénéchal, Low Temp. Phys. **32**, 424-451 (2006).
- [14] M. H. Hettler, A. N. Tahvildar-Zadeh, M. Jarrell, T. Pruschke, and H. R. Krishnamurthy, Phys. Rev. B **58**, R7475 (1998); M. H. Hettler, M. Mukherjee, M. Jarrell, and H. R. Krishnamurthy, Phys. Rev. B **61**, 12739 (2000).
- [15] Th. Maier, M. Jarrell, T. Pruschke, and M. H. Hettler, Rev. Mod. Phys. **77**, 1027 (2005).
- [16] J. E. Hirsch and R. M. Fye, Phys. Rev. Lett. **56**, 2521, (1986).
- [17] M. Jarrell and J. E. Gubernatis, Phys. Rep. **269** No.3, 133 (1996).
- [18] D. W. Hess and J. W. Serene, J. Phys. Chem. **52**, 1385 (1991).
- [19] A. Macridin, M. Jarrell, Thomas Maier, and D. J. Scalapino, Phys. Rev. Lett., **99**, 237001 (2007).
- [20] M. Vojta, arXiv:cond-mat/0803.2038 (2008).
- [21] M. B. J. Meinders, H. Eskes, and G. A. Sawatzky, Phys. Rev. B **48**, 3916 (1993).
- [22] P. Phillips, T. -P. Choy, and R. G. Leigh, preprint, arXiv:cond-mat/0802.3405 (2008).